

Long term health monitoring of post-tensioning box girder bridges

Ming L. Wang

University of Illinois - Chicago, Chicago, USA

(Received June 10, 2007, Accepted December 20, 2007)

Abstract. A number of efforts had been sought to instrument bridges for the purpose of structural monitoring and assessment. The outcome of these efforts, as gauged by advances in the understanding of the definition of structural damage and their role in sensor selection as well as in the design of cost and data-effective monitoring systems, has itself been difficult to assess. The authors' experience with the design, calibration, and operation of a monitoring system for the Kishwaukee Bridge in Illinois has provided several lessons that bear upon these concerns. The systems have performed well in providing a continuous, low-cost monitoring platform for bridge engineers with immediate relevant information.

Keywords: bridge health monitoring system; crack opening displacement (COD); bootstrap method; temperature effect.

1. Introduction

Bridges play an essential part of a highway network. They are open to traffic, resistant to natural disaster, and undaunted by millions of loading cycles per year. However, this fortitude is quite expensive to maintain and do occasionally fail (DeWolf, *et al.* 1989). The fact that many bridges are carrying greater average loads than predicted in the design has significantly increased the need to monitor bridge performance over the past few years. To effectively manage bridges today, there is a great need to monitor the real-time conditions of bridges, and the deterioration rates of their components, so that efficient and pro-active measures can be taken (Carder 1937, Catbas, *et al.* 2000, Cheung, *et al.* 1997, Ashkenazi 1997). By using the latest state-of-the-art technologies, it is possible to utilize health monitoring systems on highway bridges to determine their behavior and condition, and promote a response to maintenance and inspection needs (DeWolf, *et al.* 2002).

Bridge health monitoring systems have historically been implemented for the purpose of understanding bridge behavior under various loads and environmental effects (Bampton, *et al.* 1986, Barr 1987, Brownjohn 1994, Lau 1997, Leitch 1987, Macdonald 1997). One of the earliest documented bridge monitoring exercises was conducted on the Golden Gate and Bay Bridges in San Francisco to learn about the dynamic behavior and possible consequences of earthquakes by Carder (1937). Carder's study was applied to the probability analysis of damage caused by resonance during seismic excitation. The experimental procedure consisted of measuring ambient vibration data provided by a photographic

†Professor, E-mail: mlwang@uic.edu

seismograph that was attached to the bridge. Wind, moving water, traffic, or people working on the bridges caused the recorded vibrations. Studies of wind-induced vibration on the Golden Gate Bridge are summarized by Vincent (1958). Vincent discussed the development of a mechanical accelerometer specifically for this bridge and obtained measurements to verify that structural modifications to the bridge.

With the development of design theories and construction techniques for long-span bridges, a lot of large bridges were built during the last fifty years. For the safety of these giants, some long-term bridge monitoring systems were developed and installed. The typical examples are Commodore Barry Bridge Monitoring System (USA), Jindao Grand Bridge Monitoring System (Korea), Akashi Kaikyo Bridge Monitoring System (Japan), Alamillo Bridge Monitoring System (Spain), Hummer Bridge Monitoring System (UK), and Zhanjiang Bay Bridge Monitoring System (China), etc. In all of the long-term monitoring systems, the most extensively instrumented one is the Wind and Structural Health Monitoring System (WASHMS) for Tsingma Bridge in Hong Kong, which sensory system consists of approximately 350 sensors and their relevant interfacing units, including the latest GPS system.

However, the current long-term bridge monitoring systems lack the specific techniques to provide reliable diagnosis information of bridge condition. Most of these monitoring systems can only collect data from the sensor network and perform some simple data processing. The work of analysis and assessment has to be done manually by human specialists with the help of different independent analysis tools. For a real-time monitoring system, such as WASHMS, the huge amount of data daily collected with a high sampling rate (e.g. 100Hz) will overwhelm the bridge engineers and make the evaluation difficult and inefficient. Recent advances (Glaser, *et al.* 2007, Wang, *et al.* 2007, Nagayama, *et al.* 2007, Ni, *et al.* 2007 and Yi, *et al.* 2007) in sensor technology with data interpretation methods for decision making have a possibility to meet the challenges associated with real time structural monitoring. This paper will provide a supplement to the current research on bridge health monitoring and improve the understanding of bridge behavior.

2. Kishwaukee bridge monitoring

2.1. Backgrounds

Kishwaukee River Bridge (Rockford, IL) is a post-tensioned precast segmental concrete box-girder bridge opened to traffic in 1980. The bridge has five spans with lengths of 170 ft + 3 × 250 ft + 170 ft (51.8 m + 3 × 76.2 m + 51.8 m). As the first-generation of segmental structures, the Kishwaukee Bridge engineers chose the design of a single shear-key joint usually located close to the center of gravity of the cross section. These joints are quite vulnerable especially during polymerization of the glue.

Problem arose during and after the completion of the bridge. The epoxy applied between segments was not hardened properly in some joints. The epoxy was unable to carry fully the shear stress and was instead acting as a lubricant that caused reduction of shear resistance capacity. Therefore a substantial part of the shear force was concentrated at the shear keys (Wang 2001). As shown in Fig. 1, the inclined cracks went through only for the length of one segment but not continuously to the next segment. Many steel pins were inserted to the webs between segments to stop the propagation of shear cracks. It proves to be effective and successful slowing the progress of cracking. However, there is a need to know current shear carrying capacity as well as the extent of propagation of the cracks. A long-term monitoring program is therefore imperative for structural surveillance of Kishwaukee Bridge to provide

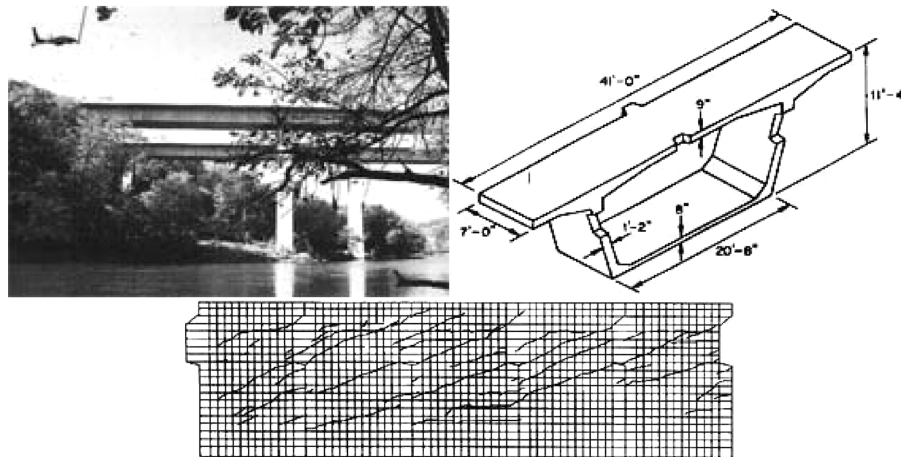


Fig. 1 Shear cracks on the webs of Kishwaukee Bridge

continuous health records for the bridge management department (Lloyd, *et al.* 2004).

Since the major problem of Kishwaukee Bridge is shear cracks on the webs, a specifically designed structural health monitoring system was installed on the Kishwaukee Southbound Bridge in 2003 (Lloyd, *et al.* 2004). This system monitors and records the strain, crack opening displacement, and acceleration of the bridge, as well as the temperature outside and inside the bridge girder. Using shear strain measured through a rosette of three crack opening displacements across cracks, its corresponding shear resistance capacity can be predicted. Thus, the operation and management for this bridge is transformed into a more objective and quantitative process. This process provides for optimal integration of experimental, analytical, and informational system components (Lloyd, *et al.* 2004). In addition, the outcome of the process provides valuable information for current evaluation of structural integrity, durability, and reliability (Lloyd 2003). Using this information, composed from the sensory system, data acquisition system, and health assessment system, the bridge owner and maintenance authorities can make rational decisions in assigning the budgets for both maintenance and repair.

2.2. Static load test

In order to determine actual health status of Kishwaukee Southbound Bridge and set up the baseline for the following long-term health monitoring, we did two static load tests in 2000. The bridge was tested for service loading conditions. The weight of the trucks was comparable with a weight of the design truck defined in AASHTO LRFD Bridge Design Specifications. The design weight of the truck (72 kips) was amplified by a dynamic factor of $\delta = 1.320$. Four different positions of the trucks were proposed on the bridge, as shown in Fig. 2.

Visual inspection of the shear cracks determined the most damaged webs in the bridge. Web SB2-N4-E was chosen for in-situ measurement of deformation due to shear forces. Three linear variable displacement transducers (LVDT) were installed at the interior surface of the web, close to the neutral axis, as shown in Fig. 3. Measured displacements were used for estimation of the web's shear stiffness. The load stage using trucks located in position #2 (second load) was selected for assessment, because neither transverse bending moments nor vertical axial stresses accompanied the imposed load in the web of segment SB2-N4. Shear forces generated by trucks located in position #3 (second load) were

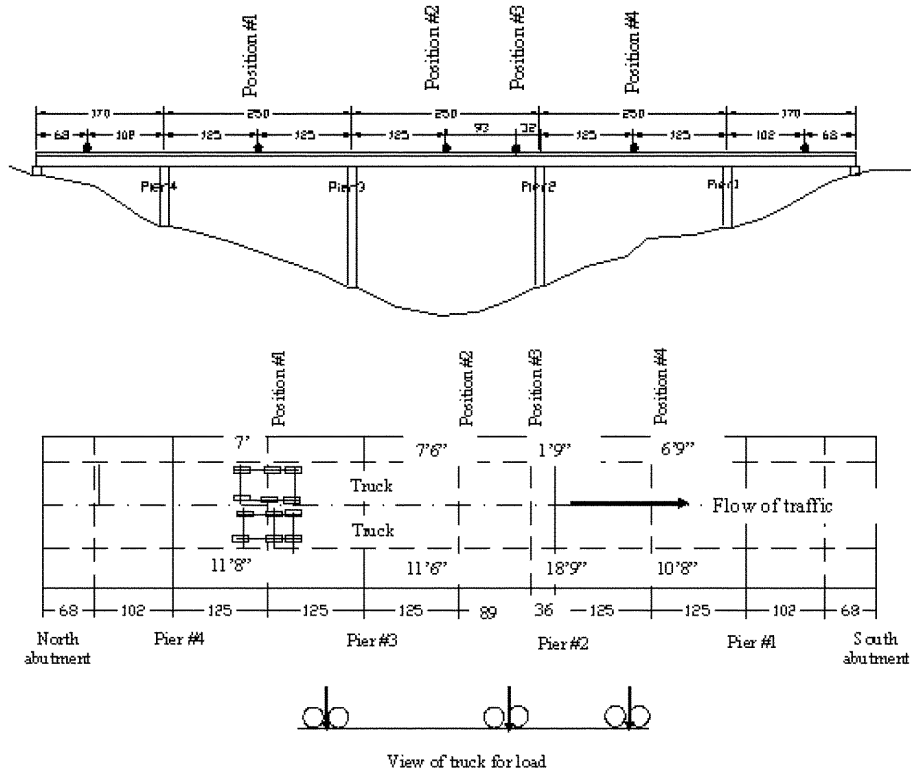


Fig. 2 Static diagnosis load test on the southbound Kishwaukee Bridge

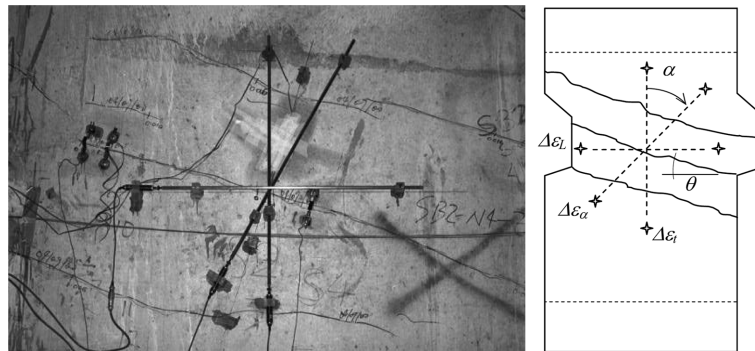


Fig. 3 LVDT sensors installed on the inner surface of the web

used for calculation of the steel stress increment in reinforcement.

Average shear strain and shear stiffness of the cracked web are expressed in Eqs. (1) and (2).

$$\Delta\gamma_{Lt} = \frac{2[\Delta\varepsilon_{\alpha} - \Delta\varepsilon_L \sin^2(\alpha) - \Delta\varepsilon_t \cos^2(\alpha)]}{2 \cos(\alpha) \sin(\alpha)} \tag{1}$$

$$(GA)_{ir} = \frac{\Delta V}{\Delta\gamma_{Lt}} \tag{2}$$

Shear stiffness can be a good indicator of steel stresses in shear reinforcement if diagram of shear flow--average shear strain $v_{Lt} - \gamma_{Lt}$ or shear stress--average shear strain $\tau_{Lt} - \gamma_{Lt}$ is known for the tested member. This diagram should be similar to diagrams such as tensile axial force vs. average axial strain $N - \epsilon_N$ or, bending moment vs. average curvature $M - \chi_M$ for RC members. The relationship $(v_{Lt} - \gamma_{Lt})$ and $(\tau_{Lt} - \gamma_{Lt})$ can be determined experimentally if tested samples have similar geometric and material properties as the investigated member.

To determine the global flexural stiffness of the bridge, strain gauges were installed at the webs of segments located next to the closures. Measured concrete strains were used for calculation of curvature in Eq. (3) and evaluation of the modulus by Eq. (4):

$$\Delta\chi_{meas} = (\Delta\epsilon_{upper} - \Delta\epsilon_{lower})/d_{gs} \tag{3}$$

$$E_c = \Delta M / (\Delta\chi_{meas} I_i) \tag{4}$$

The assessed value of modulus was still in the range from 35,000 MPa to 40,000 MPa. This value is very similar to the design value, while the tangent shear modulus has been reduced about 50-55% by shear cracks. Therefore the change of bridge shear stiffness has little influence on its flexural stiffness. Dynamic tests and FEM simulation also corroborate the negligible effect of shear stiffness on flexural stiffness.

2.3. Half-scale experiment of concrete girder

In order to determine the shear carrying capacity of Kishwaukee Bridge, a half-scale I-beam model was cast in the Lab. The following parameters are measured in this experiment: deflection of the end of cantilever; flange strains; web strains; reinforcement strains; prestressing force; elongation of the strands.

Fig. 4 presents the arrangement of the half-scale experiment. The three half-scale I-beam segments were put between the anchoring block and the dispersal segment. The friction between the joints of three segments was reduced to a certain degree to simulate the unhardened epoxy problem on the southbound Kishwaukee Bridge. The prestressing reinforcement was low relaxation strands with a high yielding point of 1800 MPa. The upper prestressing force N_1 was applied with eight 3-strand tendons on the top flange while four 4-strand tendons were used to apply the lower prestressing force N_2 on the

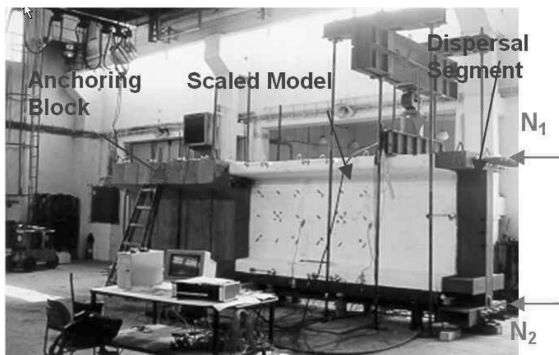


Fig. 4 Arrangement of half-scale experiment

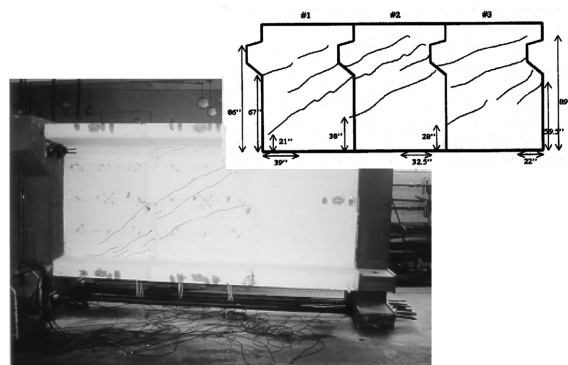


Fig. 5 Propagation of shear cracks on the *i*-beam

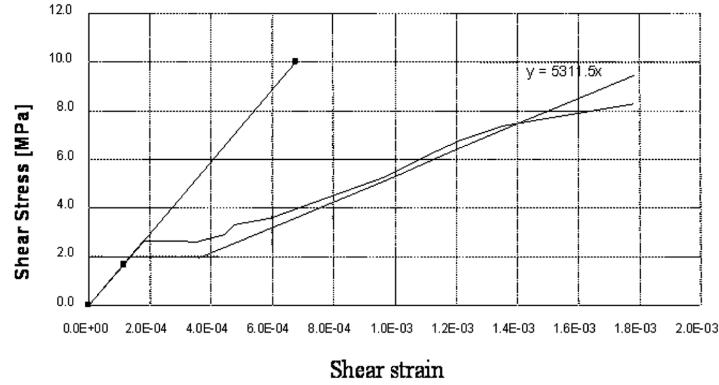


Fig. 6 Relationship of shear stress and shear strain

bottom flange. The shear force V was applied with a hydraulic jack.

The propagation of shear cracks on the I-beam webs is shown in Fig. 5. According to the visual inspection records, the type and inclination of these shear cracks are similar to the actual cracks on the Kishwaukee Bridge. It indicates the experiment successfully simulated the actual damage condition of Kishwaukee Bridge. The relationship of shear stress and shear strain is shown in Fig. 6. After the linear elastic phase, the concrete cracked and the steel reinforcement carried much of the shear force itself, which is evident from the graph. About the yielding point of shear reinforcement, the reduced tangent shear modulus was roughly 5300 MPa. According to the analysis of the static load test, the current tangent shear modulus is approximately 6740 MPa at the worst location (SB2-N4) of the southbound Kishwaukee Bridge. This means the shear reinforcements are still in the safe region of stress-strain curve. However, more strict regulations should be encouraged so that no overweight truck passes over the bridge which might induce further damage.

2.4. Bootstrap method

A L^2 -statistic for comparing two sets of random data, such as modal frequency records, is the sum of squares of the standardized test data about the population mean, $\mu_{\omega_{old}}$ (Friswell, *et al.* 1998, Lloyd, *et al.* 2000c).

$$z = \frac{1}{N_{new}} \sum_{i=1}^{N_{new}} \left(\frac{\omega_i^{new} - \mu_{\omega_{old}}}{\sigma_{\omega_{old}}} \right)^2 \quad (5)$$

The statistic z provides a basis for comparing measured outcome from two sets of modal frequencies in order to test the binary hypothesis that the mean of the test data is equal to the mean of the reference set. The failure probabilities for this statistic are defined by,

$$P_{FA} = \int_{z_c}^{\infty} f_z^{H_0}(\xi) d\xi$$

$$P_M = \int_{-\infty}^{z_c} f_z^{H_1}(\xi) d\xi \quad (6)$$

The quantities P_{FA} and P_M define the false alarm and miss probabilities, respectively. In accordance with Neyman-Pearson theory, the number z_c is a parameter chosen to fix P_{FA} at an acceptably small value (Kay 1998). In the present case, when distributions are sought for a statistic of a random process, the bootstrap is ideal since the sampling distribution of the replicate statistics converges to the parent distribution asymptotically (Efron 1979, Porter, *et al.* 1997, Hunter and Paez 1998). The bootstrap statistic that corresponds to the L^2 norm of Eq. (5) is, according to the notation in (Lloyd, *et al.* 2003a):

$$z^{def} = \frac{1}{N_{new}} \sum_{i=1}^{N_{new}} \left(\frac{\pi_i(\omega^{new}) - \hat{\mu}_{\pi_i(\omega^{old})}}{\max(\hat{\sigma}_{\pi_i(\omega^{new})}, \hat{\sigma}_{\pi_i(\omega^{old})})} \right)^2 \quad (7)$$

For $\dim(\omega)$ large, each term of the sum (distributed $\sim F$) can be approximated by the x^2 distribution. Since x^2 is replicative, the final distribution of z is approximated by,

$$\lim_{N \rightarrow \infty} f_z(z) \cong Nf_{x^2}(Nz) \quad (8)$$

The non-central statistics are more involved, and are not discussed here as, practically, the data itself should be the basis for capturing the population tail behaviour, which is crucial for estimating P_{FA} and P_M . The statistic z itself may be bootstrapped, and the results used to estimate sampling distributions of $f_z^{H_0}(\xi)$ and $f_z^{H_1}(\xi)$. Finally, the sampling distributions $\hat{f}_z(z)$ can be used to construct detector characteristic charts, at a specified level of false alarm probability, for specified N , and parameterized by some damage measure indices, that quantify the interpretation of subsequent outcomes of z .

Fig. 7 shows outcomes of this procedure for several frequency shifts of the mean (i.e. from 1.6350 (Hz)). Fig. 7(a) shows the bootstrapped sampling distributions obtained for $\omega_2^{(1)}$. The inclusion of additional modes raises N , which act directly via Eq. (5) to peak the distributions and increase the detector sensitivity (for the case $\{\omega^1, \omega^3\}$ N doubles and $z_c = 1.204$; for $\{\omega^1, \omega^2, \omega^3\}$ $z_c = 1.148$). Fig. 7(b) shows the corresponding detector behaviour for three values of N_{new} . Note that $\frac{\partial \Delta f}{\partial N} |_{P_M = 0.05} \approx -2 \times 10^{-6}$. In comparing current and reference data sets, Eq. (7) is used to calculate an outcome of z ; the decision rule is simply to accept the null hypothesis, provided $z < z_c$. In the event

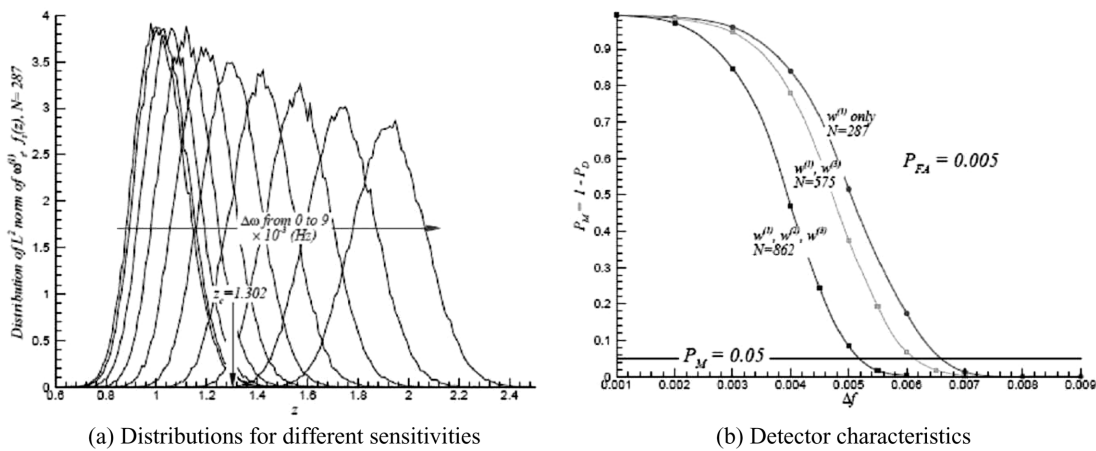


Fig. 7 Bootstrap confidence estimates obtained from reference distributions

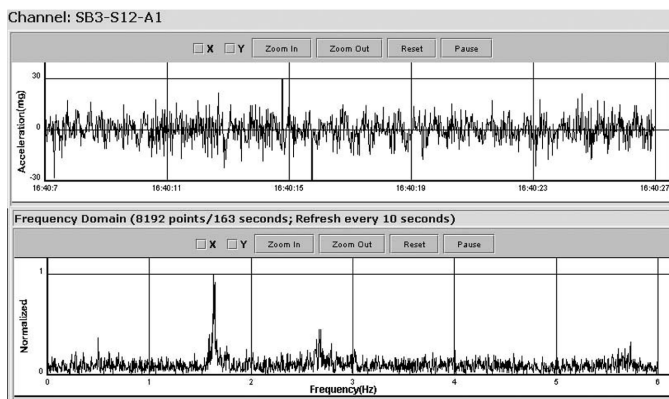
the alternative hypothesis H_1 is accepted, Fig. 7(b) provides a basis for gaging the value of Δf , constrained by any preselected value of P_M .

2.5. Real-time global and local health evaluation

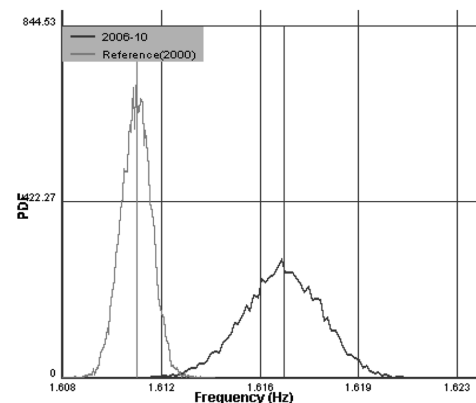
Kishwaukee bridge monitoring system has been collecting and processing data and generating evaluation and health reports for five years. The system can analyze the frequency distribution, crack opening displacement, shear strain in the web, and traffic information in real time for the Kishwaukee Bridge. Automated warning/alarm system is in effect to warn against any further local structural damage on the bridge, system problems, sensor dysfunction, and data errors.

After establishing the baseline of bridge health, a long-term monitoring system can be used to provide the continuous health information of a bridge. For concrete bridges, cracks, especially the shear cracks act as the main role of local damages. And the global health information of a bridge can be represented with the bridge stiffness. Both global and local conditions of bridges need be evaluated in order to determine their in-service behavior and justify rehabilitation and repair plans. The global health information can be provided by dynamic measurement, while the local damage can be captured by sensors such as strain gages, linear variable displacement transducer (LVDT), etc. The raw acceleration data are collected and preprocessed to obtain the natural frequencies in a sensor substation. Then the acceleration and frequency data are transferred into the database server via the internet in real time, as shown in Fig. 8(a). After that, the application server will analyze the data to get the hourly bootstrap mean and its confidence intervals, as shown in Fig. 8(b).

Based on the five dynamic tests from 1999-2000, the global dynamic characteristics of the bridge are obtained from the acceleration data with the related temperature values. Those structural parameters are setup as the baseline of global health assessment. Temperature has a significant influence on the natural frequencies of a structure. Hence it is important to derive the relationship between temperature and natural frequencies, i.e., how much the frequency will change due to the variation of 1 °C. To a certain degree, this relationship can represent the change of the bridge bending stiffness due to the temperature variation.



(a) Real-time acceleration & frequencies



(b) Bootstrap distribution of frequencies

Fig. 8 Pre-processing and post-processing of acceleration and frequencies

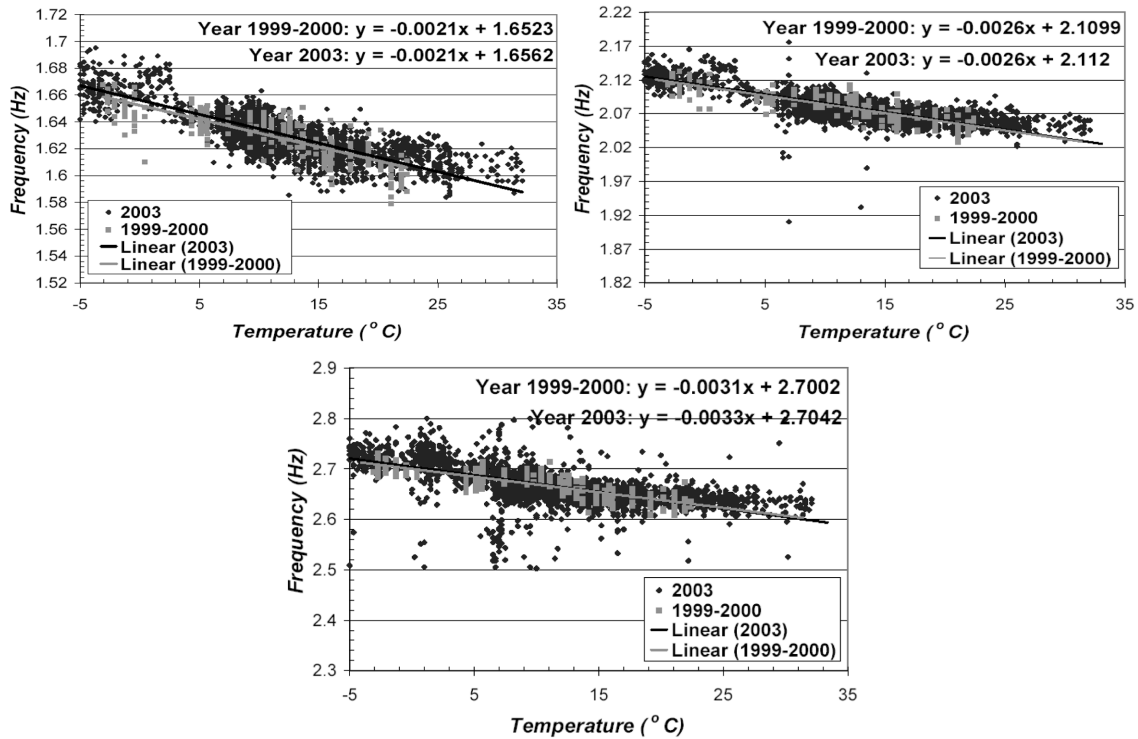


Fig. 9 Relationship between temperature and first three modes

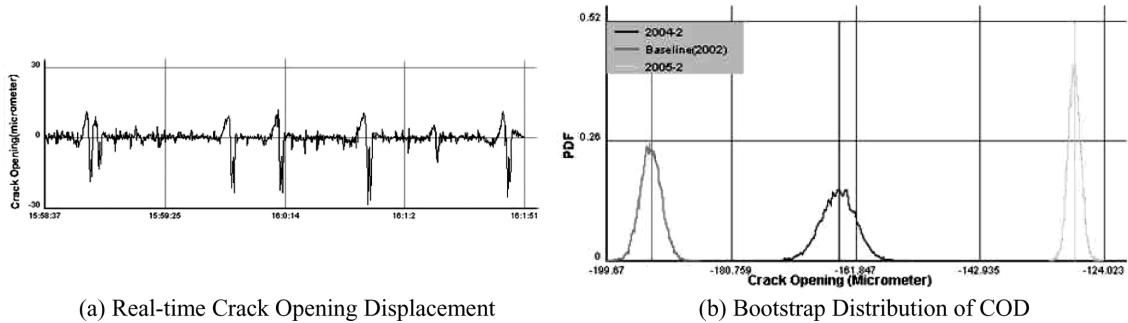
Fig. 9 provides the temperature-related regression curves and parameters of the first three modes from year 1999 to year 2004. As shown in the figure, the changes of the first two modes due to the variation of 1°C during 2004 are almost the same as the baseline (1999-2000). However, the analysis about mode 3 during year 2004 shows a little increase in the frequency change due to the unit temperature variation.

According to the theory of dynamic analysis, the changes of higher modes usually reflect the development of local damages. In order to verify the result of global health assessment and inspect the state of local damage, it is necessary to carry out the specific local health evaluation.

The raw data of crack opening displacement (COD) are preprocessed in sensor substation and transferred into the database server via the internet, as shown in Fig. 10(a). Then based on the hourly record of crack opening displacements, the application server will analyze those data to obtain their bootstrap distribution and confidence intervals. The result is shown in Fig. 10(b).

In order to find out whether the shear cracks propagated during year 2004, it is necessary to analyze the relationship between temperature and crack opening displacements, i.e., to find how much the crack opening displacement will change due to a variation of 1°C.

Based on the data of these two years, the analysis result of crack opening displacements is given in Fig. 11 according to their locations. In three years, the crack opening displacements due to temperature show some difference between the west web and the east web. As shown in the graph, on the west web, the crack opening displacement increased at the rate of about 20 micrometer per year. But on the east web of SB2-N4, the corresponding parameters are almost the same as before. The difference between the west web and the east web is possibly due to the heavier traffic on the west side of the bridge. This



(a) Real-time Crack Opening Displacement (b) Bootstrap Distribution of COD
 Fig. 10 Pre-processing and post-processing of crack opening displacement

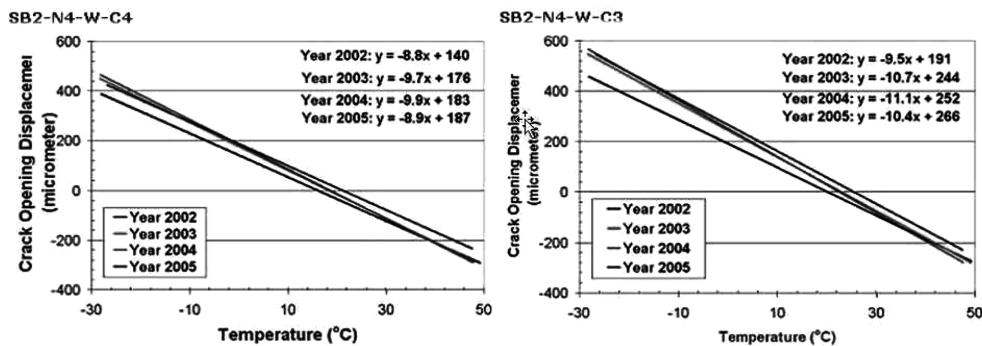


Fig. 11 Relationship between crack opening displacement and temperature

result conforms to the visual inspection of Illinois Department of Transportation. According to the analysis on crack opening displacement, we can evaluate the average shear strain of the cracking webs.

Based on the global and local measurements, the rule-based expert system gives the shear carrying capacity of the bridge with ductile mode of failure. Fig. 12(a) presents the shear stress-shear strain curve of the cracked web at Segment SB2-N4. As shown in the graph, the monthly maximum shear strain is over the baseline of the static load test in 2000. However, this value is still far below the yielding point. It indicates that the most damaged segment (SB2-N4) is still working in the nonlinear-elastic zone.

A real time bridge health monitoring system has been developed. It continuously monitors the bridge on the basis of local strain, displacement, and temperature measurements, and global frequency measurements (Lloyd, *et al.* 2003a, Lloyd, *et al.* 2003b).

The ultimate focus of the instrumentation is the measurement of permanent deformations in the web at key locations that may indicate yielding of the steel shear reinforcement and consequent changes to the load carrying capacity. This is accomplished through local and global monitoring, for maximum redundancy. The local monitoring relies on strain gage pairs installed on the web faces in the middle of each main span to estimate the loads on the bridge, and by two LVDT displacement-strain rosettes that were installed at location identified during prior static load tests as having the most severe reinforcement stresses. The global measurements are derived from ambient vibration accelerometer records.

Frequency measurements are relatively insensitive to deterioration of shear capacity. However, they are analyzed for two reasons. First, measurements were obtained by the present authors during 1999-2000 (see Fig. 13); besides visual inspections, these data are directly relevant to assessing long-term

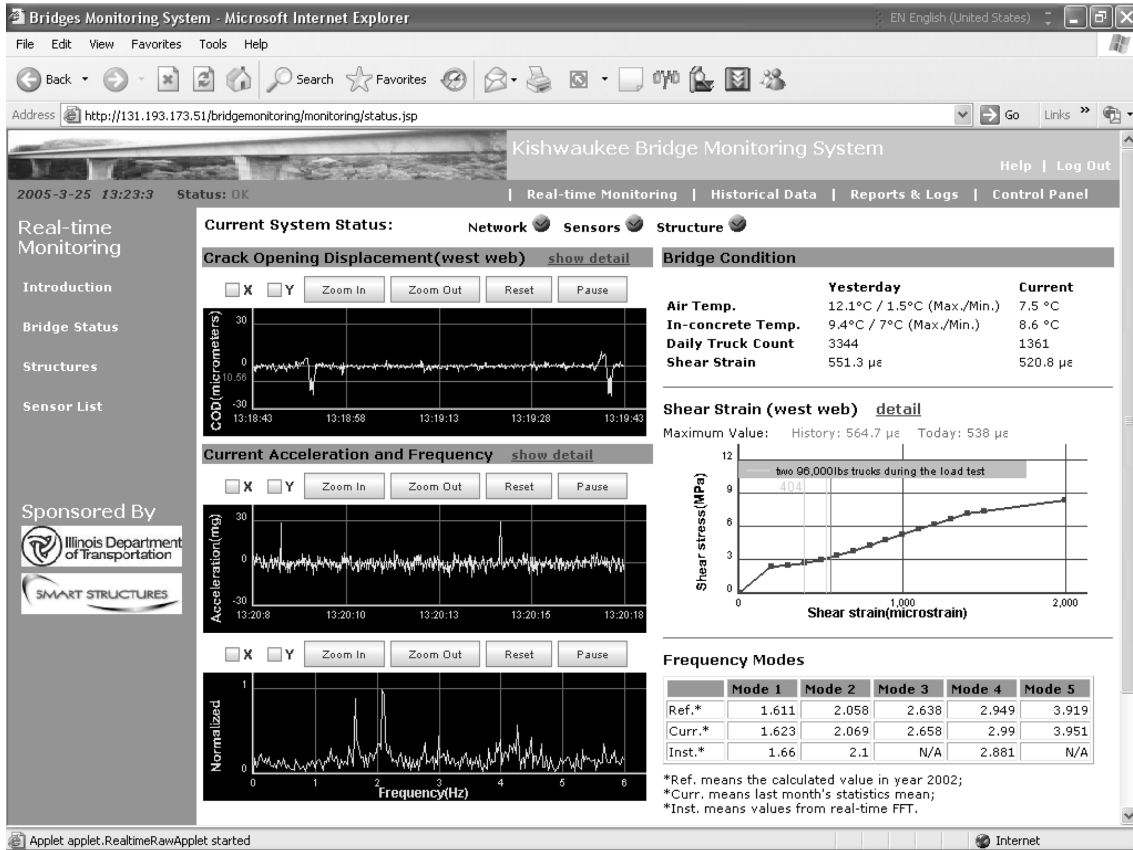


Fig. 12 Main interface page



Fig. 12(a) Shear strain (March 25, 2005)

changes in the structure (Lloyd, *et al.* 2000a), although recent experience clearly indicates the need for a more thorough understanding of thermomechanical effects (Peeters, *et al.* 2001). Secondly, both the benchmark frequency measurements and the current data are available at high resolution and accuracy, and the requisite sensitivity of frequency shifts can be explored through FEM analysis (Lloyd, *et al.* 200b). Moreover-and relevant to this paper-these two factors enable the use of bootstrap methods to develop quantitative change-point criteria for automated alarm monitoring. This is an important step, given the time and expense for manual analysis of data. These frequency data thus complement the interpretation of long-term strain and displacement measurements from moving ambient loads, data

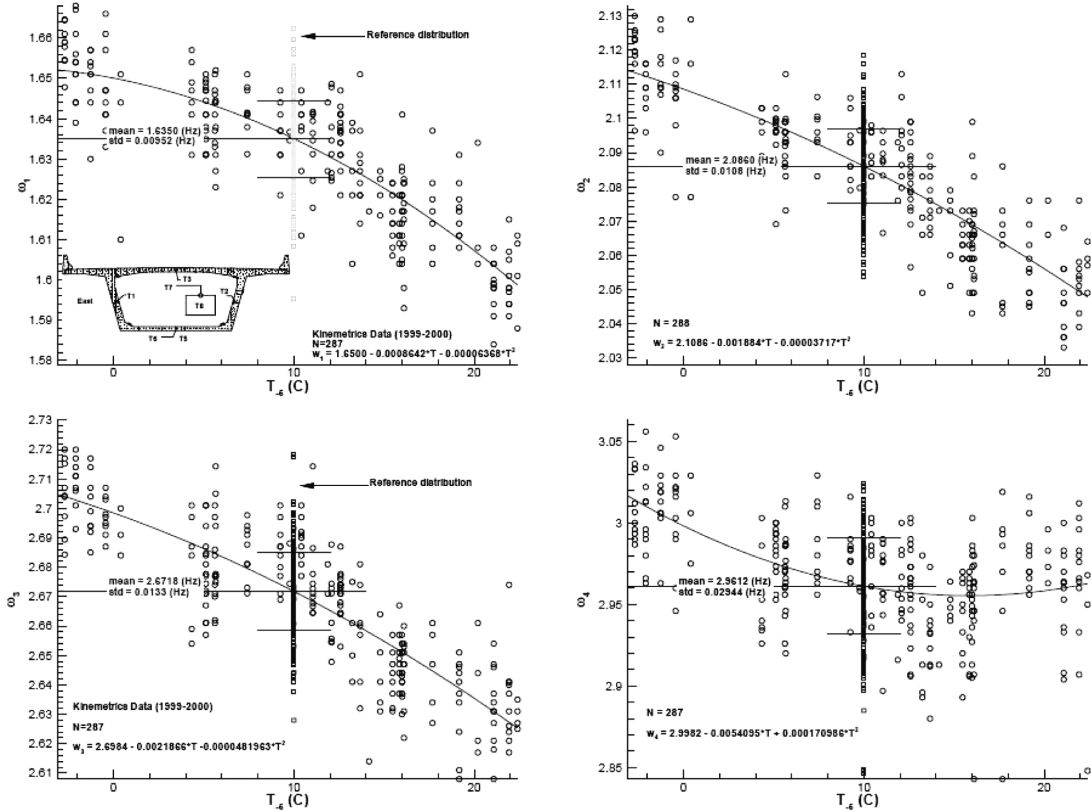


Fig. 13 Open circles denote reference frequency data obtained 1999–2000 for the South-bound Kishwaukee Bridge (primarily between 16:00 and 22:00 hours). Deterministic temperature bias inferred from T_5 (delayed five hours) was identified using least squares regression, and all frequency estimates were adjusted to a common reference temperature, $T_{ref}=10(^{\circ}\text{C})$, according to the equation, $\omega_{i,corr} = \hat{\omega}_i(T_i) - [\hat{\omega}_i(T_i) - \omega(T_{ref})]$. (Open squares denote obtained at 16:00 from 04 Dec. 2003 through Feb. 2004)

which can be beset with possible drifts and large uncertainties.

The access to the system is password protected. After entering the username and password the first page provides the basic information such as sensor status, bridge health, temperature and network connection, etc., as shown in Fig. 12. Then a selection interface gives the user choice to click on the drawing to choose the monitoring segments or choose from the menu having text description on the side bar. The user can also choose to view the real time monitoring or archived data or the expert system analysis. Fig. 12(a) shows a current shear strain value.

2.6. Temperature effect

Temperature correlation for the Fig. 13 data was performed after noting that the average lag between internal and external free air temperatures was roughly five hours. Measurements obtained from the monitoring system are available continuously and with greater precision; data studied in this paper are given in Fig. 14(a), (b). The new data allow comparison with theory to better estimate characteristic

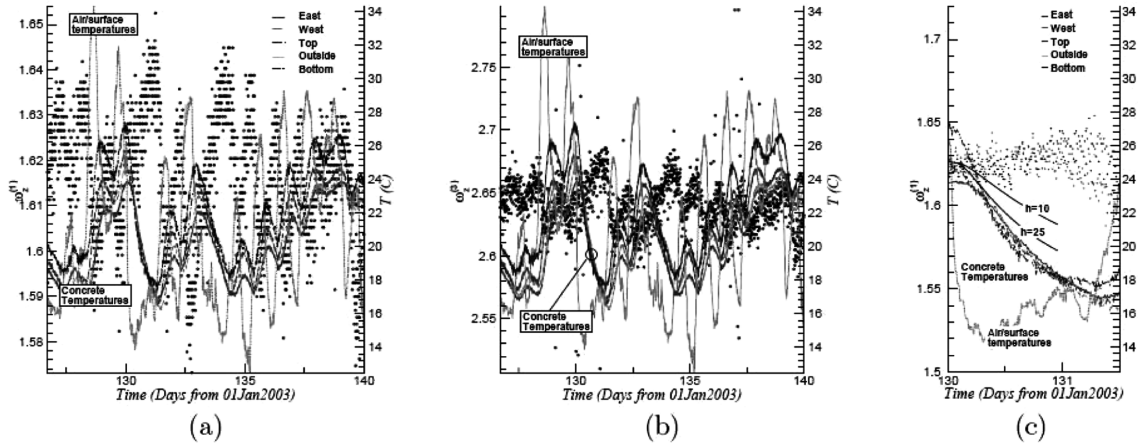


Fig. 14 FFT estimates from May 2003 (a) time variation of $\omega_z^{(1)}$ and temperatures; (b) time variation of $\omega_z^{(3)}$; (c) estimates of heat transfer coefficient based on concrete thermal properties $k = 3 \text{ W/m}\cdot\text{K}$, $\rho = 2242 \text{ kg/m}^3$, $c = 1000 \text{ J/kg}\cdot\text{K}$

thermal times and the effect of heat transfer on modal estimates. A reasonable 1d model for transient heat conduction is given by,

$$\bar{T}(x, t) = \sum_{n=1}^{\infty} c_n(\beta_n)X(\beta_n, x)e^{-Fo_n} \quad (9)$$

where \bar{T} is normalized temperature, $\beta_n = f(h, k)$ are the eigenvalues (with units of m^{-2}), Fo_n are Fourier numbers, c_n depends on a uniform initial condition of unity and $X(\beta_n, x)$ are the eigenfunctions. Heat transfer at interior surfaces is neglected.

For long times (several hours), the sum is well approximated by the first term, $\bar{T} = c_1X_1e^{-Fo_1}$ (with $c_1X_1 \sim 1-1.2$ here). Transport properties of concrete were based on suggested values (Baant and Kaplan 1996, Bentz *et al.* 1999), the largest unknown is the heat transfer coefficient h , which was estimated from data when the free stream temperature, T_s , was nominally constant, as shown in Fig. 14(c). A characteristic thermal time for a $1/e$ change to propagate through the thickness of the webs is then obtained from $Fo_n \sim \alpha\beta_1^2 \tau \equiv 1 - e^{-1}$. For the case $h = 10$, $\tau = 14.2$; for $h = 25$, $\tau = 8.4$. Corresponding times for average temperature, $\bar{T}_{avg} = L^{-1} \int_0^L \bar{T}(x, t) dx$, are 13.5 and 7.5, respectively. The corresponding values of the Biot number $Bi = hL/k \sim 1-5$ together with τ indicate the presence of large thermal gradients and stresses (Basole 1992). The analysis and new data indicate that thermal equilibrium is rare for this structure.

The critical positive thermal gradients are reviewed at 9 p.m. on July 17, 2006. Readings are shown in Fig. 15. These readings are compared to the specification (AASHTO, Guide Specifications for Design and Construction of Segmental Concrete Bridge 1999).

The crack opening has steadily increased by 110.9 micrometer in some locations since monitoring was conducted in 2002, as shown in Fig. 16. The raw LVDT data contain temperature variation as well as crack opening. It is clearly shown the trend of extension of the crack opening after elimination of the temperature effect. Accordingly, the significant conclusion which can be drawn from this observation is that the crack opening was slow, but continuous.

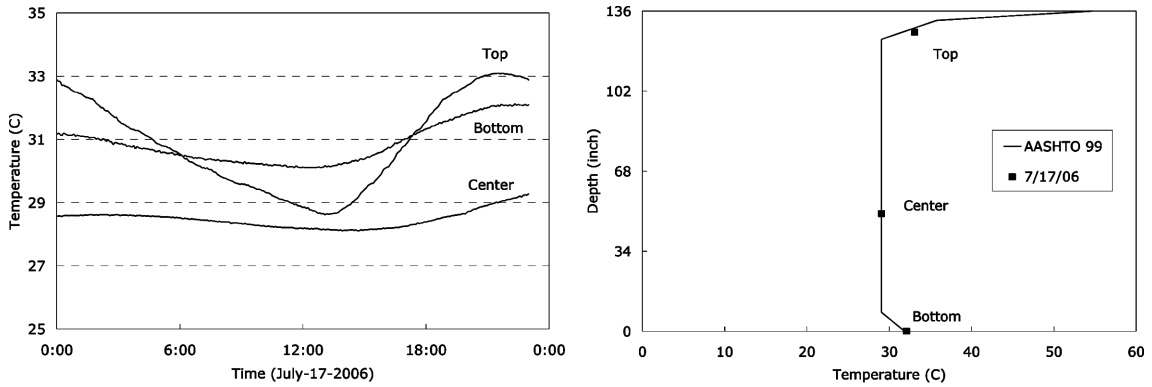


Fig. 15 Thermocouple readings and positive thermal gradient

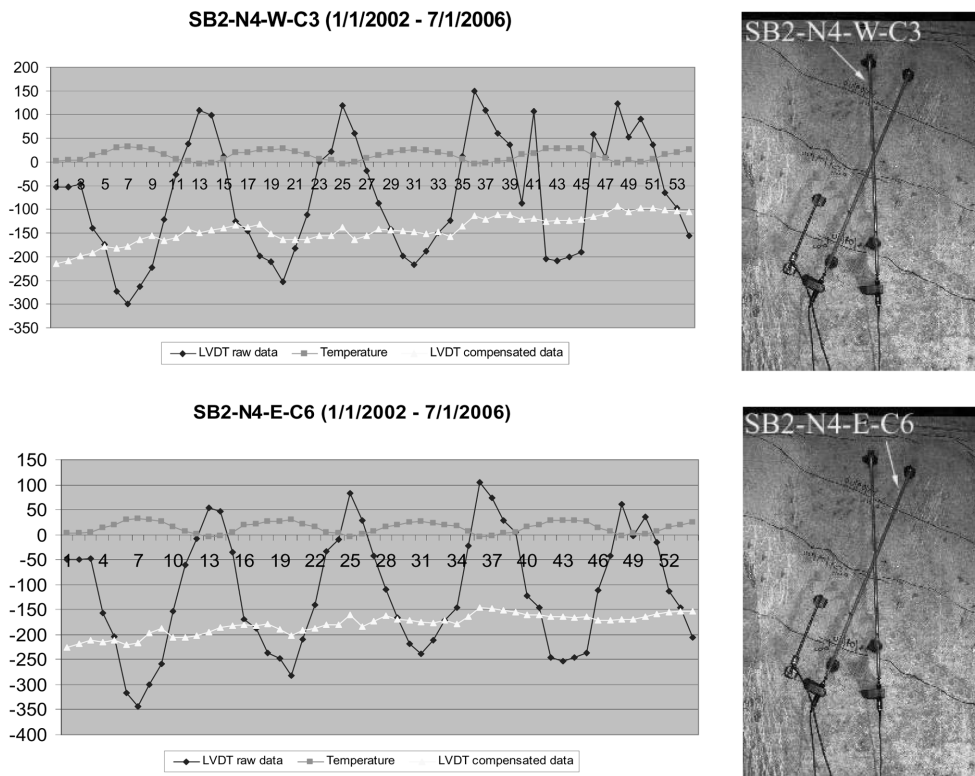


Fig. 16 Propagation of cracking with and without temperature effect

3. Conclusions

A real-time bridge monitoring system includes a real-time data acquisition, a real-time data analysis, and a health reporting system. It should provide the current health status of the bridge in real-time. It should be able to determine the current strength and resistant capacity of a structure. The key point is to use the minimum number of sensors to collect, process, and analyze the real-time dynamic and static

data from the most critical positions of the bridge.

A large-scale real-time monitoring system can generate huge amount of data every day. The excessive information will overwhelm and decrease the productivity of the bridge engineers if there is no any integrated program of data preprocessing and health diagnosis in the monitoring system. All the real-time raw data shall be pre-processed in the bridge to increase the speed of data transmission, save the capacity of database, and improve the efficiency of health assessment.

Automatic measurements should not be considered to be the be-all and end-all of bridge health monitoring. Its place is firmly entrenched in assisting engineers to conveniently carry out the damage detection, analysis, and evaluation of bridges.

Acknowledgments

The authors gratefully acknowledge the initiation and continuous support in funding from the Illinois Department of Transportation, US National Science Foundation and Smart Structure Inc. Dr. M. Chandoga and Dr. J. Halvoník at Slovak University of Technology in Bratislava is greatly appreciated.

References

- Ashkenazi, V. and Roberts, G. W. (1997), "Experimental monitoring of the Humber Bridge using GPS", *Civil Engineering, Proc ICE* **120**, 177-182.
- Břant, Z. P. and Kaplan, M. F. (1996), *Concrete at High Temperatures: Material Properties and Mathematical Models*, Longman Group Limited.
- Bampton, M. C. C., Ramsdell, J. V., Graves, R. E. and Strobe, L. A. (1986), "Deer Isle-Sedgwick suspension bridge. wind and motion analysis", Report FHWA/RD-86/183.
- Barr, I. G., Waldron, P. and Evans, H. R. (1987), "Instrumentation of glued segmental box girder bridges. Monitoring of Large Structures and Assessment of their Safety", *IABSE Colloquium Bergamo*.
- Basole, M. (1992), "Thermal modeling and field temperature measurement of segmental box girder bridges in florida", M.S. Thesis, Florida Atlantic University.
- Bentz, D. P., Clifton, J. R., Ferrais, C. F. and Garboczi, E. J. (1999), "Transport properties and durability of concrete: literature review and research plan", NISTIR 6395, U.S. Department of Commerce, September.
- Brownjohn, J. M. W., Bocciolone, M., Curami, A., Falco, M. and Zasso, A. (1994), "Humber bridge full-scale measurement campaigns 1990-1991", *JWEIA* **52**, 185-218.
- Carder, D.S. (1937), Observed vibrations of bridges. Bulletin, Seismological Society of America, **27**, 267-303.
- Catbas, F. N., Grimmelsman, K. A. and Aktan, A. E. (2000), "Structural identification of the commodore barry bridge", *Proceedings of SPIE* **3995**, 84-97.
- Cheung, M. S., Tadros, G. S., Brown, J., Dilger, W. H., Ghali, A. and Lau, D. T. (1997), "Field monitoring and research on performance of the confederation bridge", *Canadian Journal of Civil Engineering* **24**, 951-962.
- DeWolf, J., Descoteaux, T., Kou, J., Lauzon, R., Mazurek, D. and Paproski, R. (1989), "Expert systems for bridge monitoring", *Computing in Civil Engineering: Proceedings of the Sixth Conference*, p. 203-210, American Society of Civil Engineers, Atlanta, GA.
- DeWolf, J., Lauzon, R. G., Fu, Y. and Lengyel, T. F. (2002), "Long-term monitoring of bridges in connecticut for performance evaluation of structures", *Performance of Structures: From Research to Design, 2002 Structures Congress*, p. 195-196, American Society of Civil Engineers, Denver Colorado.
- Lau, C. K., Wong, K. Y. (1997), "Design, construction and monitoring of three key cable-supported bridges in hong kong", *Proc 4th International Kerensky Conference on Structures in the new millennium*, Hong Kong, 105-115.
- Leitch, J., Long, A. E., Thompson, A., Sloan, T. D. (1987), Monitoring the behaviour of a major box-girder

- bridge. Structural Assessment Based on Full and Large-Scale Testing, BRE Garston 212-219, Butterworths.
- Lloyd, G., Wang, M. L. and Wang, X. (2004), "Thermo-mechanical analysis of long-term global and local deformation measurements of the kishwaukeee bridge using the bootstrap", *Earthq. Eng. Eng. Vib.*, **3**(1), 107-115.
- Lloyd, G., Wang, M. L. and Wang, X. (2004), "Thermo-mechanical analysis of the kishwaukeee bridge from global and local deformation measurements", *Sensors and Smart Structures Technologies for Civil, Mechanical, and Aerospace Systems*, Shih-Chi Liu, Vol. **5391**, p. 618-623, SPIE, San Diego.
- Lloyd, G., Wang, M. L. and Wang, X. (2004), "Components of a real-time monitoring system for a segmental pre-cast concrete box girder bridge", *Structural Materials Technology (SMT): NDE/NDT for Highways and Bridges 2004*, Buffalo, NY.
- Lloyd, G., Wang, M. L., Wang, X. and Love, J. (2003), "Recommendations for intelligent bridge monitoring systems: architecture and temperature-compensated bootstrap analysis", *Smart Struct. Mater. 2003: Smart Systems and Nondestructive Evaluation for Civil Infrastructures*, Shih-Chi Liu, **5057**, 247-258, SPIE, San Diego.
- Lloyd, G., Wang, M. L., Wang, X. and Halvonik, J. (2003), "Bootstrap analysis of long-term global and local deformation measurements of the kishwaukeee bridge", *The 4th International Workshop on Structure Health Monitoring*, Fu-Kuo Chang, p. 163-171, Stanford University, Stanford.
- Macdonald, J. H. G., Dagless, E. L., Thomas, B. T., Taylor, C. A. (1997), "Dynamic measurements of the second severn crossing", *Proc. ICE, Transport*, **123**, **4**, 241-248.
- Miyata, T., Yamada, H., Katsuchi, H. and Kitagawi, (2002), "Fullscale measurement of akashi-kaikyo bridge during typhoon", *JWEIA* **90**, 1517-1527.
- Peeters, B., Maeck, J. and De Roeck, G. (2001), "Vibration-based damage detection in civil engineering: excitation sources and temperature effects", *Smart Mater. Struct.*, **10**, 518-527.
- Steven, D. Glaser, Hui Li, Ming L. Wang, Jinping Ou and Jerome Lynch, (2007), "Sensor technology innovation for the advancement of structural health monitoring: a strategic program of US-China research for the next decade," *Smart Struct. Sys.*, **3**(2), 221-244.
- Nagayama, T., Sim, S. H., Miyamori, Y. and Jr., Spencer, B. F. (2007), "Issues in structural health monitoring employing smart sensors", *Smart Struct. Sys.*, **3**(3), 299-320.
- Vincent, G. S. (1958), "Golden gate bridge vibration study", *ASCE J. Struct. Div.*, **84**(ST6).
- Wang, M. L., etc. (2001), "Health assessment of the kishwaukeee river bridge", Technical Report to IDOT, University of Illinois, April.
- Wang, X., Wang, M. L., Zhao, Y., Chen, H. and Zhou, L. L. (2004), "Smart health monitoring system for a prestressed concrete bridge", *Smart Structures Materials 2004: Sensors and Smart Structures Technologies for Civil, Mechanical, and Aerospace Systems*, Shih-Chi Liu, **5391**, 597-608, SPIE, San Diego.
- Wang, X. and Wang, M. L. (2002) "Smart health monitoring system of a prestressed box girder bridge", *HK Proceedings of ICANCEER 2002*, the Hong Kong Polytechnic University, Hong Kong.
- Yang Wang, R. Andrew Swartz, Jerome P. Lynch, Kincho H. Law, Kung-Chun Lu and Chin-Hsiung Loh, (2007), "Decentralized civil structural control using real-time wireless sensing and embedded computing", *Smart Struct. Sys.*, **3**(3), 321-340.
- Yi, J. H., Cho, S. J., Koo, K. Y., Yun, C. B., Kim, J. T., Lee, C. G. and Lee, W. T. (2007), "Structural performance evaluation of a steel-plate girder bridge using ambient acceleration measurements", *Smart Struct. Sys.*, **3**(3), 281-298.
- Ni, Y. Q., Ko, J. M., Hua, X. G. and Zhou, H. F. (2007), "Variability of measured modal frequencies of a cable-stayed bridge under different wind conditions", *Smart Struct. Sys.*, **3**(3), 341-356.